Available online at www.sciencedirect.com
SCIENCE DIRECT®
International Journal of Heat and Mass Transfer 47 (2004) 3797–3809
International Journal of HEAT and MASS TRANSFER
www.elsevier.com/locate/ijhmt

Drag reduction and heat transfer of surfactants flowing in a capillary tube

G. Hetsroni *, M. Gurevich, A. Mosyak, R. Rozenblit

Department of Mechanical Engineering, Technion-Israel Institute of Technology, Haifa 32000, Israel

Received 27 June 2003; received in revised form 17 March 2004
Available online 25 May 2004

Abstract

Pressure drop and heat transfer were measured in fully developed laminar flow in a pipe of inner diameter 1.07 mm in the range of Reynolds numbers $10 \leqslant Re \leqslant 450$. The study was performed for water and water–surfactant solution of 530 and 1060 ppm. It was shown that these surfactant solutions increase the pressure drop in adiabatic and diabatic flows. The dependence of friction coefficients as a function of solvent Reynolds number was used to predict the ability of certain surfactant solutions to increase drag in laminar flows.

The experimental values of the Nusselt number depend significantly on the thermal conduction through the tube wall. They become lower than theoretically predicted for tubes heated with constant heat flux on the wall.

The heat transfer coefficients with surfactant solutions were higher than that in water flow at the same bulk velocity. The results showed that the Peclet number is an additional parameter needed for a description of the averaged Nusselt number in laminar pipe flow of water and surfactant solution.

Keywords: Capillary tube; Surfactant; Laminar flow; Drag reduction; Heat transfer

1. Introduction

Recent advances in semiconductor technology have led to a significant increase in power densities encountered in micro-electronic equipment. Traditional cooling by air is not sufficient for high heat fluxes, and other means of thermal management must be considered. Among these, cooling by heat transfer to single-phase liquids flowing in small-size channels is one of the promising directions. A number of experimental and theoretical investigations have been performed and published recently, concerning various aspects of this problem. Among the subjects considered in the past, one can mention single-phase convection heat transfer in small-size channels, and dependence of these phenomena on the size and shape of the channels.

Small-size channels with hydraulic diameters on the order of 0.1–1 mm have important current and potential applications and their thermal-hydraulic characteristics have been studied recently rather extensively [1,2]. The classification of channels based on the hydraulic diameter poses considerable challenges as these channels are used in all three modes of heat transfer: single-phase, evaporation and condensation. However, for the sake of uniformity, it is desirable to have a classification scheme that is independent of the heat transfer process occurring inside the channels.

Choi et al. [3] found that measured Nusselt number in laminar flow exhibits a Reynolds number dependence, in contrast to the conventional prediction for fully developed laminar flow, in which the Nusselt number is constant. The heat transfer in channels with cross-section of 0.6×0.7 mm with forced convection was experimentally investigated by Peng and Wang [4]. They

* Corresponding author. Tel.: +972-4-8292058; fax: +972-4-8238101.
E-mail addresses: hetsroni@tx.technion.ac.il, hetsroni@techunix.technion.ac.il (G. Hetsroni).

0017-9310/$ - see front matter © 2004 Elsevier Ltd. All rights reserved.
doi:10.1016/j.ijheatmasstransfer.2004.03.009

Nomenclature

C_p	specific heat
d	pipe diameter
d_h	hydraulic diameter
f	friction coefficient
g	acceleration due to gravity
h	heat transfer coefficient
I	electric current
k	thermal conductivity of the solid wall
l	length of the test section
$\dot{m}$	mass flow rate
N	electrical power
N_1	power transferred to the fluid
N_2	power transferred axially through the tube wall
N_3	heat losses
DR	relative value
R	electric resistance of the test section
T	temperature
U	bulk flow velocity
Br	Brinkman number, $\frac{\mu U^2}{k\Delta T}$
Gr	Grashof number, $\frac{g\beta(T_{w,o}-T_{air})d_o^3}{\nu^2}$
Nu	Nusselt number, hd_i/k
Pe	Peclet number, Ud_i/α
Pr	Prandtl number, ν/α
Re	Reynolds number, Ud_i/ν

Greek symbols

α	thermal diffusivity
β	volumetric coefficient of expansion
Δ	drop (difference)
ε	emissivity
λ	thermal conductivity of the fluid
μ	dynamic viscosity
ν	kinematic viscosity
ρ	density
σ	Stefan–Boltzmann constant
τ	wall shear stress

Subscripts

air	air
cr	critical
f	fluid
fc	free convection
i	inner wall of the tube
in	inlet
IR	infrared
me	measure
o	outer wall of the tube
out	outlet
rad	radiation
sh	shear
sur	surfactant
w	wall
wat	water
x	streamwise direction

showed that the behavior of the Nusselt number on the Reynolds number was unusual. Weisberg et al. [5] and Bowers and Mudawar [6] also noted that the behavior of fluid flow and heat transfer in micro-channels, without phase change, is substantially different from that which typically occurs in conventionally sized channels. Peng and Peterson [7] suggested strong effect of geometric configuration (aspect ratio and the ratio of the hydraulic diameter to the center-to-center distance between the micro-channels) on the heat transfer and flow characteristics in single-phase laminar flow. Qu et al. [8] reported that the experimentally determined Nusselt number in the laminar regime is lower than that predicted by numerical analysis. There is no conclusive explanation of these observations up to now, although some physical phenomena (surface roughness, coupling between momentum transfer and conduction heat transfer in the liquid, natural convection, etc.) have been used to interpret these deviations from the heat transfer laws in large-scale ducts.

The low Nusselt numbers in laminar flow were attributed by Tso and Mahulicar [9,10] to the Brinkman number. Recently the heat transfer phenomenon was investigated by Gao et al. [11], Guo and Li [12], Qu and Mudawar [13]. Most of experimental data were obtained in the rectangular and trapezoidal channels or slots. This makes the interpretation of results of these investigations more complicated.

In contrast to laminar heat transfer in water flow through small-size channels and heat transfer in flow of drag reduction solutions through large-scale channels [14–21] studies on laminar flow of drag reduction solutions in mini-channels have not been reported. In addition to the usual properties such as density, specific heat, which are relatively unaffected by the presence of small amounts of surfactant, one needs to measure of shear viscosity and thermal conductivity in order to characterize the fluid. It remains unclear which basic physical properties are needed to adequately characterize the drag and heat transfer of surfactants moving in mini-channels at low Reynolds numbers.

The objective of the present study was to clarify which parameters adequately describe the pressure drop and heat transfer of surfactant solutions under fully

developed laminar pipe flow in a capillary tube. We investigated also the characteristics of the pressure drop and the heat transfer in laminar pipe flow of water and compared experimental results to those of surfactant solutions.

The cationic surfactant Habon G (molecular weight 500, Trade name Hoe S4089, Hoechst AG) was used. The cation of the surfactant is hexadecyldimethil hydroxyethyl ammonium and the counter-ion is 3-hydroxy-2-naphthoate. The experiments were carried out for water–Habon G solutions at concentration of 530 and 1060 ppm. It was shown by Zakin et al. [22,23] that although micro-structure of Habon G was mechanically degraded under high shear conditions, it recovered quickly—no matter how many times it was broken up by shear.

2. Physical properties of surfactant solutions

The measurements of the physical properties were carried out over a wide range of temperatures and for various concentrations. All solutions used were prepared by dissolving the powdered surfactant in deionized water with gentle stirring.

The shear viscosity of all surfactant solutions was determined [24] in the temperature range 25–60 °C with Rheometrics Fluids Spectrometer RFS II using a Couette system.

Figs. 1 and 2 show the effect of shear rate on shear viscosity for a 530 and 1060 ppm of Habon G solutions at different temperatures. One can see that, at low shear rates, the shear viscosity of the Habon G solution is significantly higher than that of clear water. The curves come closer to one another for higher shear rates. The magnitude of the shear viscosity as a function of the shear rate decreases, when the temperature of the solution increases.

The thermal conductivity (Fig. 3) was measured by Hetsroni et al. [24]. It was shown that thermal conductivity of the surfactant solutions did not differ from that of the solvent (water). The density and specific heat were taken to be those of the solvent, since the concentration did not exceed 1060 ppm.

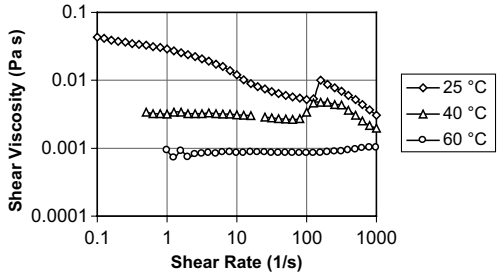

Fig. 1. Dependence of shear viscosity of Habon G solution (530 ppm) on shear rate.

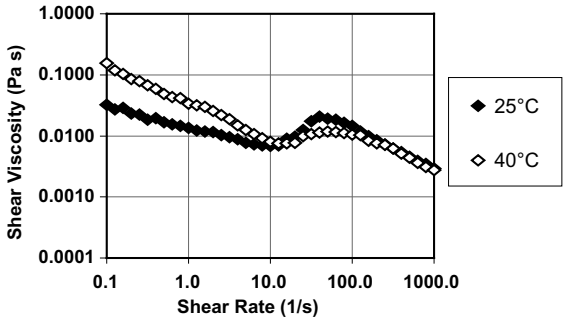

Fig. 2. Dependence of shear viscosity of Habon G solution (1060 ppm) on shear rate.

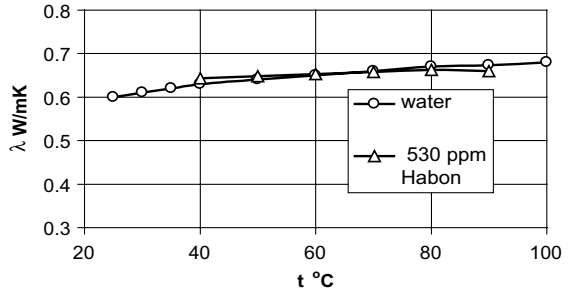

Fig. 3. Dependence of thermal conductivity vs. temperature.

3. Experimental

3.1. Experimental apparatus

The experimental apparatus is shown in Fig. 4a and b. Water was flowing from the entrance tank 2 and was supplied to the capillary tube by a peristaltic pump 3. The flow rate was measured by weighing method using the electronic scales 1. The tested tube of inner diameter 1.07 mm, outer diameter 1.5 mm and 0.600 m in length was placed horizontally. It is divided into two sections. The development section 5 is 0.245 m in length. It was used for the flow and thermal field development. The test section 6 of 0.335 m in length was used for collecting the experimental data on heat transfer and pressure drop.

The details of the experimental setup are shown in Fig. 4b. The test section was not insulated, because the outer temperature of the heated wall, $T_{w,o}$, was measured by IR radiometer. On the other hand, the insulation of small-size diameter tube is meaningful, if the critical diameter of insulation $d_{CR} = 2k/h_{fc}$ is less than a tube diameter. The estimation of the value of the critical diameter of an insulation gives the magnitude of $d_{CR} =$ 13.3 mm, at the heat transfer coefficient of the free convection is $h_{fc} = 15$ W/m^2 K and heat conductivity of

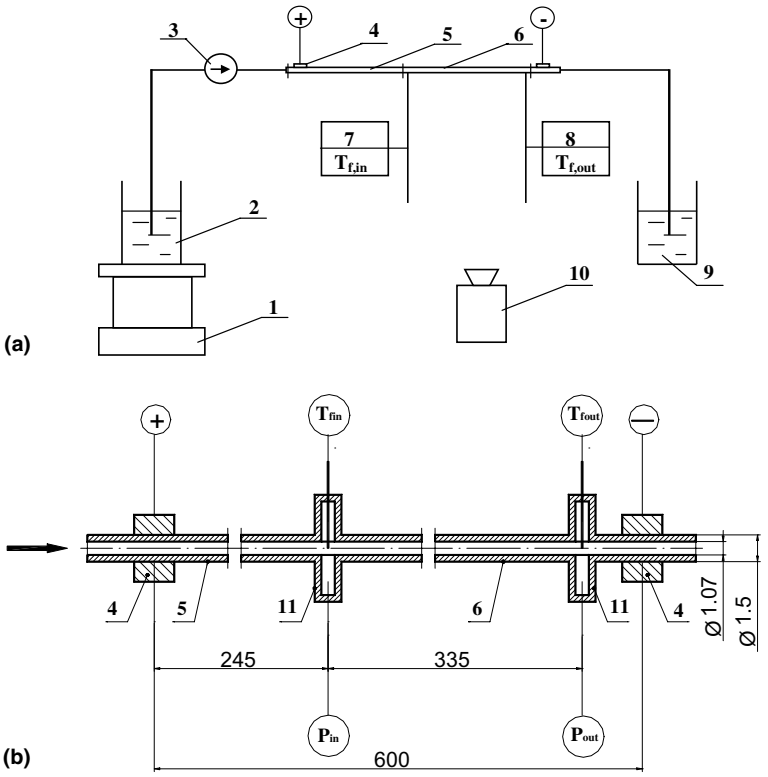

Fig. 4. Experimental apparatus. (a) schematic diagram of the experimental facility: (1) electronic scales, (2) entrance tank, (3) pump, (4) contacts of power supply, (5) development section, (6) test section, (7) thermocouple for measurement of inlet fluid temperature, (8) thermocouple for measurement of outlet fluid temperature, (9) exit tank, (10) infrared camera, (11) junction; (b) test section.

this insulation is $k = 0.1$ W/m K. So, in our case, a small tube diameter (1.5 mm) without any insulation assures much less heat losses than a thick layer of the high-quality insulation.

The inlet and outlet of this test section were connected to junctions 11. The pressures in the junctions were measured by silicon pressure sensors with sensitivity 3.3 mV/kPa and response time 1.0 ms. The measured pressure drop included also a minor loss due to a sudden change of the cross section. The inlet and outlet temperatures of the working fluid were measured by 0.3 mm type T thermocouples 7 and 8, calibrated with an accuracy of ±0.1 K. The DC current was supplied by a power supply through electrical contacts 4 to direct heating the stainless steel tube. The flow rate of the working fluid was controlled by adjusting the frequency of the peristaltic pump and was measured by a weighing method. Then the water was collected at the exit tank 9. The temperature field on the test section surface was recorded by Infrared radiometer 10.

The infrared radiometer used in this experiment had a spectral band of 3.4–5 μm. The radiometer is cryogenically cooled, and has a temperature range of −10 to 450 °C with a sensitivity of 0.07 at 30 °C. The radiometer has a 256×256 platinum silicide focal plane array detector, which provides a superior image without the use of mechanical scanning. Image update range is 50 Hz. Through calibration, the radiometer is very accurate in a narrow temperature range giving typical noise equivalent temperature difference (NETD) only, which is less than the sensitivity. A typical horizontal resolution is 1.2 mRad or 256 pixels/line. IR dynamic range is 16 bits and digitizing resolution is 12 bits (4096 levels). Focus range is from 20 cm to infinity.

3.2. Methodology of temperature measurement on the heated surface

Measurement of the temperature field of micro-object by infrared radiometer is quite difficult. The small tube diameter allows considerable background radiation. If the background has a temperature different from that of the small-sized object, the surface temperature of the device will have substantial error. Microscopic lenses drastically confine the length of the tube, which can be observed but do not eliminate completely the influence of the background temperature. The special method (Hetsroni et al. [25]), similar to the method of the dis-

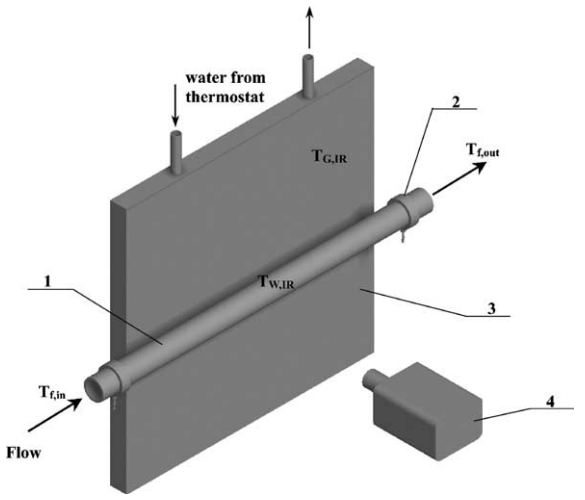

Fig. 5. Method of wall temperature measurement: (1) test section, (2) electrical contacts, (3) background, (4) infrared camera.

appearing filament at color temperature measurement, was used to avoid the effect of the background noise. The method is based on compensating the background radiation by controlling its temperature to the level equal to the measured temperature on test mini-tube surface. This is achieved by recording the infrared data against a background, whose temperature was maintained at a given value by a thermostat, Fig. 5. The surface temperature, $T_{w,o} = T_{w,IR}$, of the test section is determined from the infrared image, which is recorded by IR radiometer against the background. The background temperature, $T_{G,IR}$, was also measured by the radiometer. Both the object and the background screen were made of the same stainless steel and were painted by the same black paint, so that the test section and the background had equal emissivity.

For verification of the method a series of experiments were conducted. In these experiments the temperature of the background was measured as by IR radiometer as well as by calibrated, T-type thermocouples of diameter 0.3 mm. When the temperature of background was equal to the temperature on the surface of test tube the object temperature could be measured with accuracy ±0.3 K (95% confidence level) [25].

3.3. Data reduction

The total heat balance of the test section may be expressed as

$$N = N_1 + N_2 + N_3 \tag{1}$$

where N is the power generated by Joule heating, N_1 is the power transferred to the fluid, N_2 is the power conducted axially by the tube wall, N_3 are the heat losses.

The power generated by Joule heating was calculated as

$$N = I^2 R \tag{2}$$

The electric resistance of the test section was calculated according to the wall temperature of the capillary pipe as

$$R_T = R_0[1 + \alpha_R(T - T_0)] \tag{3}$$

where R_T and R_0 are the values of the resistance at temperature T and T_0, respectively and α_R is the temperature coefficient of resistivity. The initial temperature T_0 is taken as 20 °C.

The power transferred to the fluid moving in the pipe

$$N_1 = \dot{m}C_p(T_{f,out} - T_{f,in}) \tag{4}$$

The average Nusselt number and the average heat transfer coefficient, h_{fc}, for the free convection from the horizontal tube was calculated by expression given by Churchill and Chu [26] for $10^{-5} < GrPr < 10^{12}$

$$Nu^{1/2} = 0.60 + 0.387\left(\frac{GrPr}{[1 + (0.559/Pr)^{9/16}]^{16/9}}\right)^{1/6} \tag{5}$$

The heat losses from the test section to the environment due to free convection depend on the outer wall temperature, $T_{w,o}$ and the environmental temperature, T_{air}. They were calculated as

$$N_{3,fc} = h_{fc}(T_{w,o} - T_{air})\pi dl \tag{6}$$

The heat losses from the test section to the environment due to radiation were calculated as

$$N_{3,rad} = \varepsilon\sigma(T_{w,o}^4 - T_{air}^4)\pi dl \tag{7}$$

where $\varepsilon = 0.95$ is the emissivity of the test section, σ is the Stefan–Boltzmann constant.

$$N_3 = N_{3,fc} + N_{3,rad} \tag{8}$$

and

$$N_2 = N - N_1 - N_3 \tag{9}$$

The heat flux q to the fluid is obtained as

$$\frac{q = \dot{m}C_p(T_{f,out} - T_{f,in})}{\pi dl} \tag{10}$$

where $\dot{m}$ is the mass flow rate, C_p is specific heat, d is inner tube diameter and l is length of the test section.

The average values of the heat transfer coefficient is defined as

$$\bar{h} = \frac{q}{(\overline{T}_{w,i} - \overline{T}_f)} \tag{11}$$

where $\overline{T}_{w,i}$ is the average surface temperature of the inner tube wall and $\overline{T}_f$ is the average value of the fluid

temperature, defined as $\overline{T}_f = (T_{f,in} + T_{f,out})/2$. The temperature of the inner tube wall was calculated from the temperature of the outer tube wall and the heat generated per unit of volume of an electrically heated tube [24]. All thermophysical properties of water, needed for evaluation of average values of Nu and Re numbers, were determined at this average temperature.

The Reynolds number $Re_{sh} = Ud_i/v_{sh}$ is based on the shear viscosity of the solution, defined as $8U/d_i$ [27]. The Reynolds number $Re_{wat} = Ud_i/v_{wat}$ is based on the kinematic viscosity of water.

The measured pressure drop ΔP_{me} accounts for the pressure drop along the capillary tube, ΔP, as well as the pressure losses associated with abrupt expansion and contraction at the tube inlet and outlet, ΔP_{in} and ΔP_{out}, respectively. An expression for the pressure drop across the tube is

$$\Delta P = \Delta P_{me} - \Delta P_{in} - \Delta P_{out} \tag{12}$$

A relative pressure drop, $DR(\Delta P)$, can be defined as

$$DR(\Delta P) = (1 - \Delta P_{sur}/\Delta P_{wat}) \tag{13}$$

where ΔP_{sur} and ΔP_{wat} are pressure drops of the of surfactant solutions and water respectively, at the same bulk velocity.

Relative friction coefficient, $DR(f)$, can be defined as

$$DR(f) = (1 - f_{sur}/f_{wat}) \tag{14}$$

where f_{sur} and f_{wat} are friction coefficients of the flow of surfactant solutions and water (at the same Reynolds number), respectively. The friction coefficient was calculated according to the relation $f = 2\tau/\rho U^2$, where τ is wall shear stress, i.e.

$$f = \frac{1}{2}\Delta P \frac{d}{l}\frac{1}{\rho U^2} \tag{15}$$

Relative heat transfer coefficient, $DR(h)$

$$DR(h) = (1 - h_{sur}/h_{wat}) \tag{16}$$

where h_{sur} and h_{wat} are heat transfer coefficients in the tube at the same bulk velocity of surfactant solutions and water, respectively.

Relative Nusselt number, $DR(Nu)$

$$DR(Nu) = (1 - Nu_{sur}/Nu_{wat}) \tag{17}$$

where Nu_{sur} and Nu_{wat} are the Nusselt numbers at the same Reynolds number of surfactant solutions and water, respectively.

3.4. Experimental uncertainty

The temperature of the heated outer wall, $T_{w,o}$, was measured with an accuracy 0.3K (95% confidence level). The uncertainty of the components for an estimation of an error measurement of wall temperature was obtained according to the standard 1995 Guide to the Expression of Uncertainty of the Measurements (1995 GEUM) [28]. The details of calculation are presented by Hetsroni et al. [25]. The error in determining the Nusselt number, Nu, formed from an estimation of errors that became at measurements of the following values: d—the diameter of the test section; l—the length of the test section; $\dot{m}$—mass flow rate; $(T_{out} - T_{in})$—difference between outlet and inlet temperatures of the liquid; $(T_{wi} - T_f)$—difference between the averaged value of the inner wall and the liquid temperatures as well as an error in the magnitude of the physical properties as C_p—specific heat of water and λ—thermal conductivity of water.

The error of the product fRe is

$$\delta(fRe)/(fRe) = [(\delta\Delta P/\Delta P)^2 + (4\delta d/d)^2 + (\delta l/l)^2 + (\delta m/m)^2]^{0.5} \tag{18}$$

Eq. (18) shows that the channel hydraulic diameter measurement introduces essential error into the uncertainty of the product fRe.

The error in determining the power, N, generated by Joule heating is due to errors of measurements of both the electric current and the electric resistance. The error in magnitude of the power transferred to the working fluid into the tube, N_1, is due to uncertainties of flow rate, m, specific heat of water, C_p, difference between outlet and inlet liquid temperatures, $T_{out} - T_{in}$. The error in the estimation of heat losses, N_3, is due to correlations for calculation of natural convection and radiation heat transfer.

The error in determining N_2 depends on errors of N, N_1 and N_2. Performing the error analysis according to [28] the uncertainties in determining various parameters in this study given in Table 1.

4. Experimental results and discussion

4.1. Dependence of the pressure drop on the bulk velocity

Drag reduction is a reduction in the pressure drop of the turbulent flow in a pipe at the same bulk velocity (or flow rate) due to additives, Toms [29]. We used this terminology in the present section for both adiabatic and diabatic laminar flow in capillary tube.

4.1.1. Adiabatic flow

A plot of the pressure drop depending on the bulk velocity (or flow rate) in adiabatic flow is shown in Fig. 6a. The data were obtained at constant temperature of the fluids $T_f = 25$ °C. It can be seen, the pressure drop for 530 and 1060 ppm Habon G solutions increases compared to that of the solvent (water). Result of this test shows that certain surfactant may increase the pressure drop in adiabatic laminar pipe flow.

Table 1
Experimental uncertainties (95% confidence level)

NN	Source of uncertainty	Symbol	Uncertainty, %
1	Diameter of the test section	d	1.0
2	Length of the test section	l	0.3
3	Wall temperature	T_w	0.4
4	Difference between inlet and outlet temperatures of liquid	$T_{in} - T_{out}$	2.0
5	Difference between wall and liquid temperatures	$T_w - T_f$	3.0
6	Mass flow rate	$\dot{m}$	3.0
7	Electrical power	N	1.5
8	Power transferred to fluid	N_1	3.3
9	Power transferred through tube wall	N_2	12.5
10	Heat losses	N_3	12
11	Heat transfer coefficient	h	13.0
12	Nusselt number	Nu	13.1
13	Friction coefficient	f	10.2
14	Reynolds number (based on the water properties)	Re	4.5
15	Specific heat of water	C_p	0.05
16	Thermal conductivity	λ	0.5
17	Kinematic viscosity of water	v	2.1
18	Thermal conductivity of surfactant	λ_s	4
19	Shear viscosity of surfactant	v_{sh}	4
20	Reynolds number based on the shear viscosity	Re_{sh}	5.5

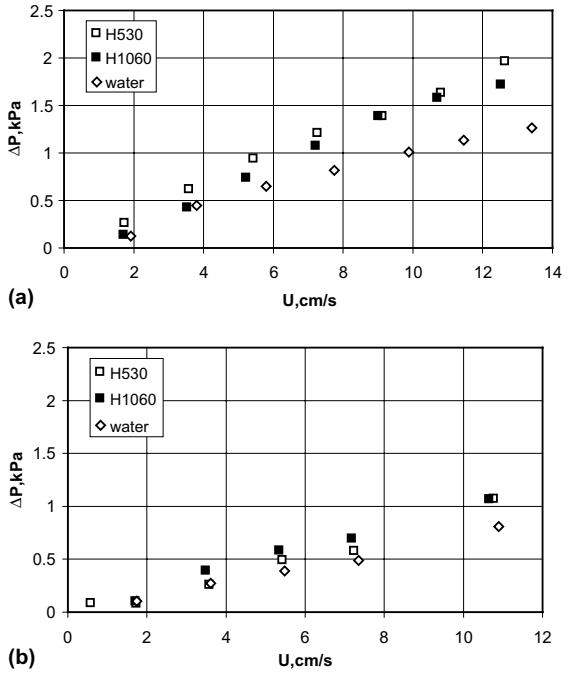

Fig. 6. Dependence of pressure drop on fluid bulk velocity: (a) adiabatic flow; (b) diabatic flow.

We also measured the temperature of the fluid at the entrance and the exit of the test section. The outlet and the inlet temperatures were equal within experimental uncertainty of 0.1 K. In the present experiments, the increase in the fluid temperature due to a viscous dissipation was negligible.

4.1.2. Diabatic flow

It should be mentioned that shear viscosity depends on the temperature of the surfactant solution. The drag reduction and heat transfer deterioration should be compared at the same temperature of the solution. For this reason the pressure drop was measured in the same range of solutions temperatures, in which the heat transfer experiments were performed. Fig. 6b shows pressure drop in the diabatic flow. The fluid was flowing into the tube which was directly heated by an electric current. The temperature of the fluid increased along the test section approximately from 40 to 60 °C. This test also indicates that the pressure drop for Habon G solutions increases compared to clear water (Fig. 6b).

4.2. Dependance of the friction factor on the Reynolds number

4.2.1. Friction factor

Most pressure drop measurements are typically evaluated as a function of the friction factor vs. the Reynolds number. The drag reduction phenomenon can also be interpreted as the additives reduce the wall shear stress. The wall shear stress and the Fanning's friction factor are determined by Eq. (15). Lumley [30] proposed a definition of drag reduction in turbulent flow: drag reduction is the reduction of friction below that of the solvent. We applied this definition to laminar flow. The behavior of the friction factor vs. the Reynolds number

is often used to describe the drag reduction phenomenon. The Reynolds number includes the kinematic viscosity value. An additive of even small amount of some surfactant to water changes the shear viscosity of the solution (Fig. 2) relative to that of the solvent. As we have also seen, the viscosity of the surfactant solution depends on the shear rate, and this is one of main problems in describing the behavior of the friction factor. Below we discuss the pressure drop measurements evaluated as a dependence on both solution-based and solvent-based Reynolds numbers.

4.2.2. Friction coefficients as a function of solution Reynolds numbers

Fig. 7a and b show friction factors, f, as a function of the Reynolds numbers, Re_{sh}, based on the shear viscosity for adiabatic and diabatic flows, respectively. For both 530 and 1060 ppm Habon G solutions the friction factors are lower than that for a Newtonian fluid in a pipe with smooth walls, where the friction factor is $f = 16/Re_{sh}$. These are some unexpected results. As it may be concluded from Fig. 6a and b, the Habon G solutions are not drag reducing in laminar flow. Dependence f vs. Re_{sh} does not reflect this phenomenon. The Reynolds number based on shear velocity is not valid to describe drag reduction in laminar flow. According to Lumley's [30] definition the flows have to be compared using the same viscosity, given by the one of the solution. It has become customary to use the kinematic viscosity of the solvent with respect to the definition of the friction factor as a function of the Reynolds number [15,22,31–33].

4.2.3. Friction coefficients as a function of the solvent Reynolds number

Fig. 8a and b show friction factors as a function of the Reynolds numbers, Re_{wat}, based on the water viscosity for adiabatic and diabatic flows, respectively. The line $f = 16/Re_{wat}$ is also presented in this figure. These Figures reflect the relation of friction coefficients to drag reduction and one can conclude that at the same Reynolds numbers higher values of friction coefficients correspond to higher values of pressure drop.

4.2.4. Drag reduction

Fig. 9a and b show the relative pressure drop, $DR(\Delta P)$, plotted as a function of fluid bulk velocity, U, in adiabatic and diabatic flow, respectively. The data were calculated using Eq. (13). These results (the negative values of $DR(\Delta P)$) illustrate that in surfactant solutions the relative pressure drop is independent of bulk fluid velocity and it is about 50% higher than that of clear water.

Fig. 10a and b present relative friction factor, $DR(f)$, plotted as a function of the Reynolds number based on shear viscosity of the solutions, Re_{sh}, in adiabatic and diabatic flow, respectively. These data represent the percent of drag reduction calculated using Eq. (14). They show positive values of drag reduction, which are depended on Reynolds number, Re_{sh}. It seems that using

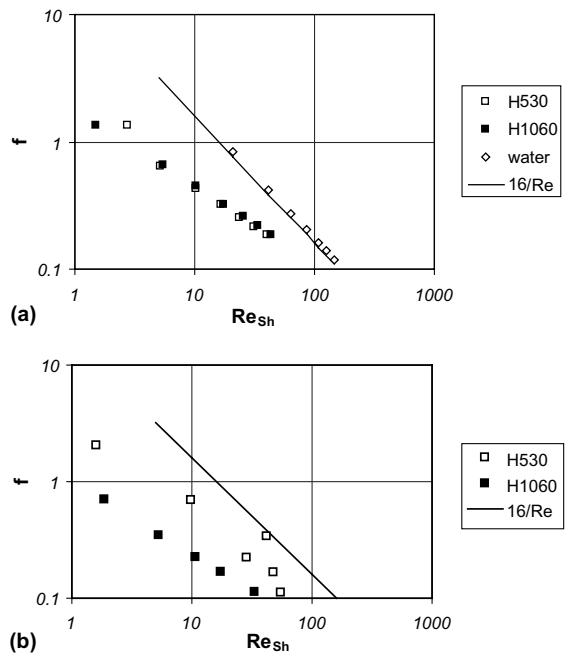

Fig. 7. Friction coefficients as a function of solution Reynolds number Re_{Sh}: (a) adiabatic flow; (b) diabatic flow.

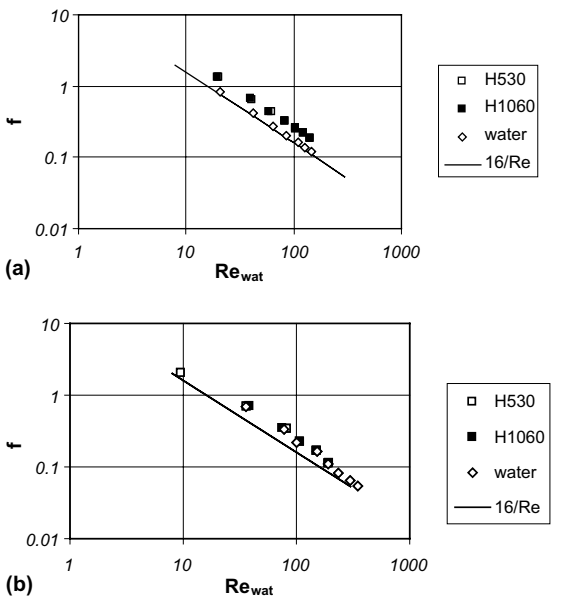

Fig. 8. Friction coefficients as a function of solvent Reynolds number Re_{wat}: (a) adiabatic flow; (b) diabatic flow.

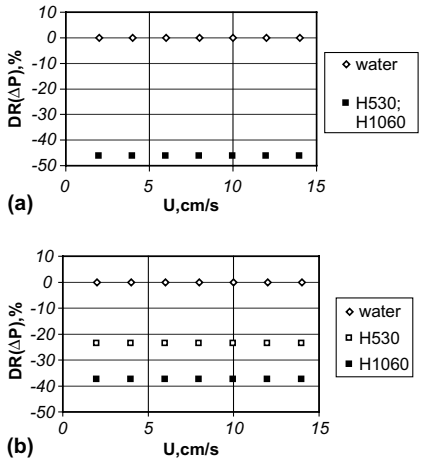

Fig. 9. Relative pressure drop as a function of liquid bulk velocity: (a) adiabatic flow; (b) diabatic flow.

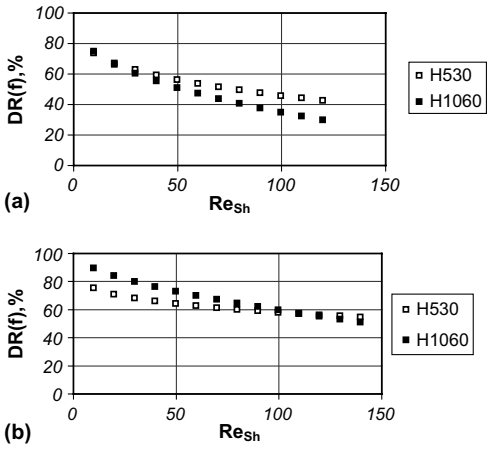

Fig. 10. Relative friction coefficients as a function of solution Reynolds number Re_{Sh}: (a) adiabatic flow; (b) diabatic flow.

the Reynolds number based on solution properties, Re_{sh}, leads to confusion of an interpretation of the experimental data in terms of the usual drag at the same flow rate. For example, the measurements carried out in the present study (see Fig. 9a and b) indicate that at given flow rate the pressure drop in Habon G solutions increases, while the dependence $\mathrm{DR}(f)$ vs. Re_{sh} shows decrease in the friction factor compared to water flow at the same Re_{sh}.

4.3. Heat transfer in water flow

4.3.1. Average heat transfer coefficients

We studied also the behavior of the average Nusselt number depending on the Reynolds number. These experiments were carried out in the range of Reynolds

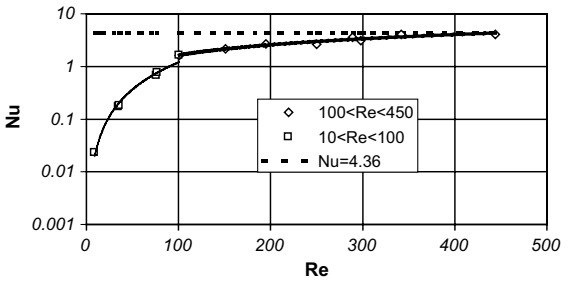

Fig. 11. Dependence of the average Nusselt number on the Reynolds number (water flow).

number $Re = 10$–450. The dependence of the Nusselt number, Nu, on the Reynolds number, Re, is presented in Fig. 11.

As seen in the Fig. 11, the experimental values of Nu are lower than the theoretical values of Nusselt number for the tubes heated with a constant heat flux. Such a behavior qualitatively agrees with one reported by Choi et al. [3]. Qu et al. [8] conducted experiments to investigate heat transfer characteristics of water flowing through trapezoidal silicon micro-channels with a hydraulic diameter ranging from 62 to 169 μm. The experimental results were compared with the numerical predictions and a significant difference was found. A comparison between the results indicated that the experimentally determined Nusselt number is much lower than that given by the numerical analysis. Qu et al. [8] assumed that measured lower Nusselt numbers might be due to the effect of surface roughness on walls of the micro-channels. Based on the roughness–viscosity model a modified relation was proposed to interpret the experimental results. This model showed no Nusselt number dependence on the Reynolds number For $100 < Re < 1400$. Contrary to these findings Qu and Mudawar [13] demonstrated that the conventional Navier–Stokes and energy equations could adequately predict the fluid flow and heat transfer in rectangular micro-channels 231 μm wide and 713 μm deep.

Gao et al. [11] reported an increase in the Nusselt number, Nu, with increase in the Reynolds number, Re, measured for the smallest flow rates corresponding to the Reynolds numbers up to about 250. The experimental Nusselt numbers for all micro-channels are approximately constant in the range $250 < Re < 1500$. Such a behavior of Nusselt numbers at low Reynolds numbers ($Re < 250$) was attributed by Tso and Mahulicar [9,10] to the Brinkman number. Our experiments did not show substantial effect of Brinkman number on behavior of Nusselt number in the range of $10 < Re < 450$.

In general, the axial heat conduction in the channel wall of a conventional size of channels can be neglected because the wall thickness is usually very small compared

to the channel diameter. Shah and London [34] found that the Nusselt number for developed laminar flow in the tube fall between 4.36 and 3.66, which corresponds to Nusselt numbers for constant heat flux and constant temperature boundary conditions, respectively. However, for flow in micro-channels, the wall thickness can be of the same order of channel diameter and may affect the heat transfer significantly. For example, Choi et al. [3] reported that the average Nusselt numbers in micro-channels with hydraulic diameters from 9.7 to 81.2 μm were much lower than for conventional channels and increased with increasing Reynolds number. Results of the present study are in qualitative agreement with data of Choi et al. [3].

The heat transfer interaction between the fluid and solid depends on the geometrical and thermophysical properties of the solid wall. Fig. 12a–c show the dependence of relations N_1/N, N_2/N and N_3/N on the Peclet number, Pe, (where N_1 is the heat transferred to the fluid, N_2 is the heat conducted axially through the tube wall, N_3 is the heat losses and N is electrical power supplied to heat the tube). The relation of N_2/N becomes very high at low Peclet numbers. Comparison between the results presented in Fig. 12b and those presented in Fig. 11 allows one to conclude that the effect of thermal conduction through the solid wall leads to decrease in the Nusselt number. This effect decreases with increasing in the Reynolds number.

It should be noted, that in previous experimental investigations of heat transfer in small-size channels the axial heat flux was neither measured nor estimated. In general, the axial heat conduction in the channel wall can be neglected for conventional size of channels. In capillary tube the axial heat flux affects both the temperature of the heated wall and the bulk fluid temperature distribution along the flow direction. Usually the fluid temperature in mini-tubes was linearly interpolated between temperatures measured at the inlet and outlet collectors of the experimental setup. However Herwig and Hausner [35] showed that the bulk fluid temperature does not change linearly in the streamwise direction in micro-channels at low Reynolds numbers.

4.4. Heat transfer in flow of surfactant solutions

4.4.1. Average heat transfer coefficients

Dependence of average heat transfer coefficient, h, on fluid bulk velocity, U, is plotted in Fig. 13. This figure shows that the heat transfer coefficient in surfactant solutions is higher than in laminar pipe water flow. Fig. 14 shows relative enhancement in heat transfer coefficient DR(h) vs. fluid bulk velocity, U (it should be noted, that the negative values of DR(h) shown in Fig. 14 correspond to an increase in the heat transfer coefficient). It can be seen from Fig. 14 that the increase in the heat transfer coefficient does not depend of solution

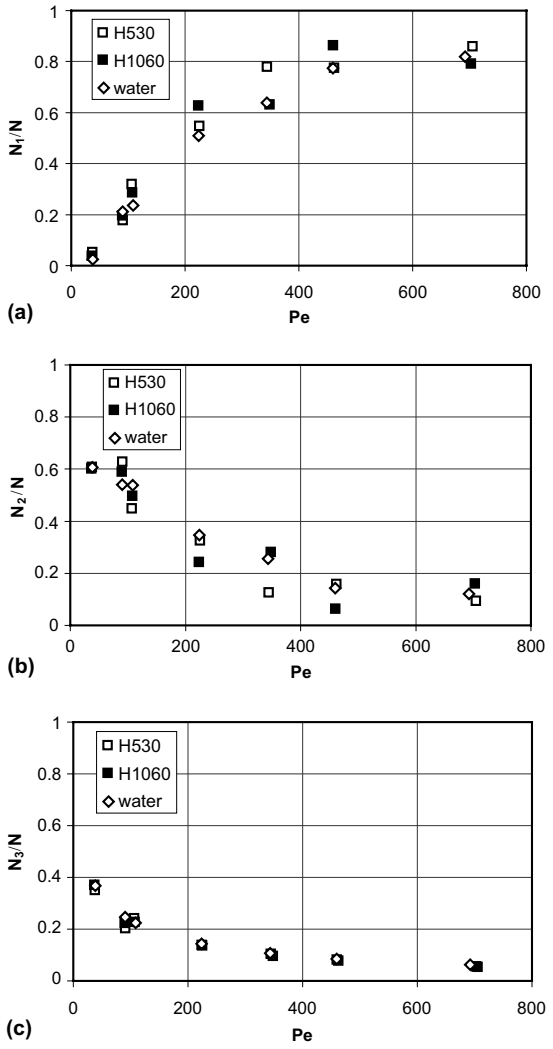

Fig. 12. Dependence of relations N_1/N, N_2/N and N_3/N on the Peclet number.

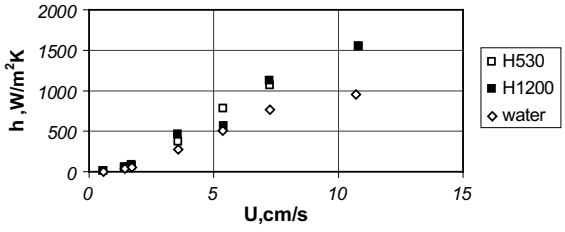

Fig. 13. Average heat transfer coefficient depending on the liquid velocity.

bulk velocity. As the addition of surfactant macromolecules to water increases the viscosity and pressure drag in laminar pipe flows, it is quite unexpected to find that

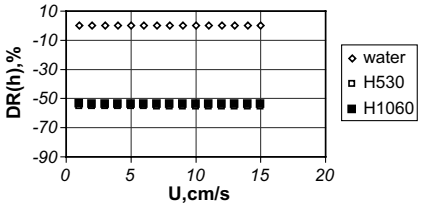

Fig. 14. Relative heat transfer coefficient on liquid velocity.

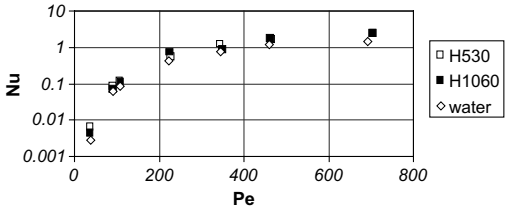

Fig. 16. Dependence of the Nusselt number on the Peclet number.

for heat transfer the opposite can sometimes take place. Kostic [17] observed that some drag-reducing solutions augmented the heat transfer in laminar flow through a non-circular duct. They suggested that the fluid elasticity may lead to secondary flows, which are responsible for the increase heat in the transfer. The secondary flows increase the pressure drops in both adiabatic and diabatic flows. However, in diabatic flow the total pressure drop (due to friction and due to secondary flows) may be smaller compared to that in adiabatic one. In this case the common effect includes also some decrease in the fluid viscosity with an increase in the temperature of the surfactant solution. This tendency is shown in Fig. 9a and b. On the other hand, it may be assumed that macromolecules of surfactant change the flow structure in the near wall region. It also may be responsible for the increase in pressure drop and heat transfer.

Dependence of averaged Nusselt number, Nu, on shear Reynolds number, Re_{sh}, is presented in Fig. 15. The Nu vs. Re_{sh} is qualitatively similar to water behavior for all surfactant solutions used. At given value of Reynolds number, Re_{sh}, the Nusselt number, Nu, increases with an increase in the shear viscosity. As discussed above, the use of shear viscosity for the determination of drag reduction is not a good choice. The heat transfer results also illustrate the need of using more appropriate physical parameter. In particular, Fig. 15 shows that the Nusselt number increases in laminar pipe flow more then 10 times compared to that of water, while the increase in the heat transfer coefficient did not exceed 60%.

Fig. 16 shows dependence of the Nusselt number on the Peclet number. The Nusselt numbers of all solutions

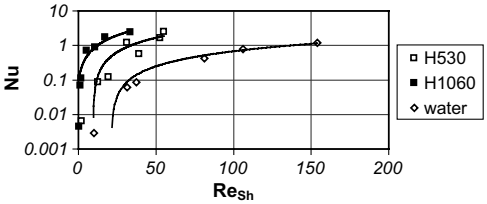

Fig. 15. Dependence of the averaged Nusselt number on the solution Reynolds number.

are in agreement with heat transfer enhancement presented in Fig. 14. The present experiments show that the use of the Peclet number may be considered for a description of the experimental data in laminar pipe flow of certain non-Newtonian fluids.

5. Conclusions

The experiments on pressure drop and heat transfer were carried out in fully developed laminar pipe flow, in a capillary tube, for the both water and surfactant solutions of 530 and 1060 ppm Habon G. The dependence of the pressure drop on the bulk velocity showed that these surfactant solutions increase the pressure drop in adiabatic and diabatic flows. An increase in the fluid temperature due to viscous dissipation was not observed.

The dependence of the friction coefficients on the solvent Reynolds was used to predict an ability of certain surfactant solutions to increase of the drag in laminar flows. The Reynolds number based on shear velocity is not valid to describe this phenomenon.

The experimental values of the Nusselt number in water flow were significantly lower than theoretical predicted for tubes heated at constant heat flux. It was established that the effect of thermal conduction along the solid wall leads to a decrease in the Nusselt number, if a linear change of the fluid temperature in the flow direction is assumed. Experiments carried out in the pipe of inner diameter of 1.07 mm did not show substantial effect of Brinkman number on the behavior of the Nusselt number in the range $10 < Re < 100$.

The heat transfer coefficients in Habon G surfactant solutions were higher than that in water flow at the same bulk velocity. The results showed that the Peclet number is an additional parameter needed for a description of the averaged Nusselt number in laminar pipe flow of water and surfactant solutions.

Acknowledgements

This research was supported by the Technion VPR Fund. A. Mosyak and R. Rozenblit are supported by a

joint grant from the Center for Absorption in Science of the Ministry of Immigrant Absorption and the Committee for Planning and Budgeting of the Council for Higher Education under the framework of the KAMEA PROGRAM.

References

[1] S.M. Ghiaasiaan, S.I. Abdel-Khalik, Two-phase flow in microchannels, Adv. Heat Transfer 34 (2001) 145–253.
[2] S.G. Kandlikar, Fundamental issues related to flow boiling in mini-channels and microchannels, Keynote lecture at the ExHFT-5 conference held in Salonika, Greece, 24–28 September 2001.
[3] S.B. Choi, R.R. Barren, R.Q. Warrington, Fluid flow and heat transfer in micro-tubes, ASME DSC 40 (1991) 89–93.
[4] X.F. Peng, B.X. Wang, Forced convection and flow boiling heat transfer for liquid flowing through microchannels, Int. J. Heat Mass Transfer 36 (1993) 3421–3427.
[5] A. Weisberg, H.H. Bau, J. Zemel, Analysis of microchannels for integrated cooling, Int. J. Heat Mass transfer 35 (1992) 2465–2474.
[6] M.B. Bowers, I. Mudawar, High flux boiling in low flow rate, low pressure drop mini-channel and microchannel heat sinks, Int. J. Heat Mass Transfer 37 (1994) 321–332.
[7] X.F. Peng, G.P. Peterson, The effect of thermofluid and geometrical parameters on convection of liquids through rectangular microchannels, Int. J. Heat Mass Transfer 38 (1995) 755–758.
[8] W. Qu, Gh.M. Mala, D. Li, Heat transfer for water in trapezoidal silicon micro-channels, Int. J. Heat Mass Transfer 43 (2000) 3925–3936.
[9] C.P. Tso, S.P. Mahulikar, The use of the Brinkman number for single phase forced convective heat transfer in microchannels, Int. J. Heat Mass Transfer 41 (1998) 1759–1769.
[10] C.P. Tso, S.P. Mahulikar, Experimental verification of the role of Brinkman number in microchannels using local parameters, Int. J. Heat Mass Transfer 43 (2000) 1837–1849.
[11] P. Gao, S. Le Person, M. Favre Marinet, Hydrodynamics and heat transfer in a two-dimensional microchannel, in: Proceedings of the 12th International Heat Transfer conference, Grenoble, France, 18–23 August 2002.
[12] Z.Y. Guo, Z.X. Li, Size effect on micro-scale single phase flow and heat transfer, in: Proceedings of the 12th International Heat Transfer conference, Grenoble, France, 18–23 August 2002.
[13] W. Qu, I. Mudawar, Experimental and numerical study of pressure drop and heat transfer in a single-phase microchannel heat sink, Int. J. Heat Mass Transfer 45 (2002) 2549–2565.
[14] P.S. Virk, Drag reduction fundamentals, AIChE J. 21 (1975) 625–656.
[15] Y.I. Cho, J.P. Hartnett, Non-Newtonian fluids in circular pipe flows, Adv. Heat Transfer 15 (1982) 60–141.
[16] J.P. Hartnett, M. Kostic, Heat transfer to Newtonian and non-Newtonian fluids in rectangular ducts, Adv. Heat Transfer 19 (1989) 247–356.
[17] M. Kostic, On turbulent drag and heat transfer reduction phenomena and laminar heat transfer enhancement in non-circular duct flow of certain non-Newtonian fluids, Int. J. Heat Mass Transfer 37 (1994) 133–147.
[18] C.X. Lin, S.Y. Ko, F.K. Tsou, Laminar heat transfer in square duct flow of aqueous CMC solutions, Int. J. Heat Mass Transfer 39 (1996) 503–510.
[19] G. Aguilar, K. Gasljevic, E.F. Matthys, Coupling between heat and momentum transfer mechanisms for drag reducing polymer and surfactant solutions, J. Heat Transfer 121 (1999) 796–802.
[20] K. Gasljevic, G. Aguilar, E.F. Matthys, An improved diameter scaling correlation for turbulent flow of drag-reducing polymer solutions, J. Non-Newtonian Fluid Mech. 84 (1999) 131–148.
[21] G. Aguilar, K. Gasljevic, E.F. Matthys, Asymptotes of maximum friction and heat transfer reductions for drag-reducing surfactant solutions, Int. J. Heat Mass Transfer 44 (2001) 2835–2843.
[22] J.L. Zakin, J. Myska, Z. Chara, New limiting drag reduction and velocity profile asymptotes for nonpolymeric additives systems, AichE J. 42 (1996) 3544–3546.
[23] J.L. Zakin, Y. Qi, Y. Zhang, in: Proceedings of 15th International Congress of Chemical and Process Engineering, CHISA 2002, Prague, Czech Republic, 25–29 August 2002.
[24] G. Hetsroni, J.L. Zakin, Z. Lin, A. Mosyak, E.A. Pancallo, R. Rozenblit, The effect of surfactants on bubble grows, wall thermal patterns and heat transfer in pool boiling, Int. J. Heat Mass Transfer 44 (2001) 485–497.
[25] G. Hetsroni, M. Gurevich, A. Mosyak, R. Rozenblit, Surface temperature measurement of a heated capillary tube by means of an infrared technique, Measur. Sci. Technol. 14 (2003) 807–814.
[26] S.W. Churchill, H.H.S. Chu, Correlating equations for laminar and turbulent free convection from a horizontal cylinder, Int. J. Heat Mass Transfer 18 (1975) 1049.
[27] F.N. Cogswell, Polymer Melt Rheology: A Guide for Industrial Practice, Woodhead Publishing Limited, Cambridge, 1981.
[28] Guide to the Expression of Uncertainty of Measurement, Geneva, International Organization for Standardization, 1995.
[29] B.A. Toms, Some observations on the flow of linear polymer solutions through straight tubes at large Reynolds numbers, in: Proceedings of International Congress on Rheology, vol. 2, North Holland, Amsterdam, 1949, pp. 135–141.
[30] J.L. Lumley, Drag reduction by additives, Ann. Rev. Fluid. Mech. (1969) 367–384.
[31] A. Gyr, H.W. Bewersdorff, Drag Reduction of Turbulent Flows by Additives, Kluwer Academic Publishers, Dordrecht, Boston, London, 1995.
[32] P.S. Virk, H.S. Mickley, K.A. Smith, The ultimate asymptote and mean flow structure in Toms' phenomenon, ASME J. Appl. Mech. 37 (1970) 488–493.

[33] M.D. Warholic, G.M. Schmidt, T.J. Hanratty, The influence of a drag-reducing surfactant on a turbulent velocity field, J. Fluid Mech. 388 (1999) 1–20.
[34] R.K. Shah, A.L. London, Laminar flow forced convection in ducts, in: T.F. Irvine, J.P. Hartnett (Eds.), Advances in Heat Transfer, (Supplement 1), Academic Press, New York, San Francisco, London, 1978.
[35] H. Herwig, O. Hausner, Critical view on "new results in micro-fluid mechanics" an example, Int. J. Heat Mass transfer 46 (2003) 935–937.